

Lepton flavor violating Higgs decay $h \rightarrow \mu\tau$ in the littlest Higgs Model with T-parity

Bingfang Yang^{1,*} Jinzhong Han^{2,†} and Ning Liu^{1‡}

¹*College of Physics and Materials Science,
Henan Normal University, Xinxiang 453007, China*

²*School of Physics and Telecommunications Engineering,
Zhoukou Normal University, Henan, 466001, China*

Abstract

Inspired by the recent CMS $h \rightarrow \mu\tau$ excess, we calculate the lepton flavor violating Higgs decay $h \rightarrow \mu\tau$ in the littlest Higgs model with T-parity (LHT). Under the constraints of $\ell_i \rightarrow \ell_j\gamma$, $Z \rightarrow \ell_i\bar{\ell}_j$ and Higgs data, we find that the branching ratio of $h \rightarrow \mu\tau$ can maximally reach $\mathcal{O}(10^{-4})$. We also investigate the correlation between $h \rightarrow \mu\tau$, $\tau \rightarrow \mu\gamma$ and $Z \rightarrow \mu\tau$, which can be used to test LHT model at future e^+e^- colliders.

PACS numbers: 14.65.Ha, 12.15.Lk, 12.60.-i

*Electronic address: yangbingfang@htu.edu.cn

†Electronic address: hanjinzhong@zknu.edu.cn

‡Electronic address: wlln@mail.ustc.edu.cn

I. INTRODUCTION

The discovery of the Higgs boson at the Large Hadron Collider (LHC) [1] is a great step toward understanding the electroweak symmetry breaking (EWSB) mechanism. To ultimately establish its nature, a precise study of the Higgs boson properties, in particular the Higgs rare decays and productions [2], will be important tasks at LHC and future colliders.

In fact, CMS 8 TeV data has shown a 2.4 excess in searching for Higgs mediated lepton flavor violation (LFV) process $h \rightarrow \tau\mu$, which is interpreted to the branching ratio: $\text{Br}(h \rightarrow \mu\tau) < 1.51 \times 10^{-2}(\text{CMS})$ [3]. While ATLAS only observed a small excess in one of the signal regions and reported an upper limit: $\text{Br}(h \rightarrow \mu\tau) < 1.43 \times 10^{-2}(\text{ATLAS})$ [4]. From the available data it is premature to draw any definite conclusion and more data is needed to confirm its existence. However, the lepton flavor violating decay of the Higgs boson is widely predicted in various extensions of the Standard Model (SM), such as seesaw[5], supersymmetric (SUSY)[6], two-Higgs doublet model (2HDM)[7], 3-3-1 model[8], and other ones[9]. In the SM, the LFV process is extremely suppressed by Glashow-Iliopoulos-Maiani (GIM) mechanism[10] due to the smallness of neutrino mass. So, any observation of such decays would indicate the new physics beyond the SM.

As an extension of the SM, the littlest Higgs Model with T-parity(LHT) is one of the popular candidates that can successfully solve the hierarchy problem. The LHT model predicts many new particles, such as heavy gauge bosons, mirror fermions, heavy scalars and heavy top partners. Moreover, the flavour structure of the LHT model is richer than the one of the SM, mainly due to the presence of the mirror fermions and their weak interactions with the ordinary fermions. It has been shown that the LHT model can give significant contributions to some LFV processes [11]. In this work, we investigate the LFV process $h \rightarrow \mu\tau$ in the LHT model under the current constraint of $\ell_i \rightarrow \ell_j\gamma$, $Z \rightarrow \ell_i\bar{\ell}_j$ and Higgs data.

The paper is organized as follows. In Sec.II we give a brief review of the LHT model related to our work. In Sec.III we calculate the LFV process $h \rightarrow \mu\tau$ in unitary gauge under current constraints. In Sec.IV we investigate the correlation between $h \rightarrow \mu\tau$, $\tau \rightarrow \mu\gamma$ and $Z \rightarrow \mu\tau$ in the LHT model. Finally, we draw our conclusions in Sec.V.

II. A BRIEF REVIEW OF THE LHT MODEL

The LHT model is based on an $SU(5)/SO(5)$ non-linear σ model[12], where the $SU(5)$ global symmetry is broken down to $SO(5)$ at the scale $f \sim \mathcal{O}$ (TeV) by the vacuum expectation value (VEV) of the σ field, Σ_0 , given by

$$\Sigma_0 = \langle \Sigma \rangle \begin{pmatrix} \mathbf{0}_{2 \times 2} & 0 & \mathbf{1}_{2 \times 2} \\ 0 & 1 & 0 \\ \mathbf{1}_{2 \times 2} & 0 & \mathbf{0}_{2 \times 2} \end{pmatrix}. \quad (1)$$

The VEV Σ_0 also breaks the gauged subgroup $[SU(2) \times U(1)]^2$ of the $SU(5)$ down to the SM electroweak $SU(2)_L \times U(1)_Y$. After EWSB, the new T-odd gauge bosons W_H^\pm, Z_H, A_H acquires masses, given at $\mathcal{O}(v^2/f^2)$ by

$$M_{W_H} = M_{Z_H} = gf(1 - \frac{v^2}{8f^2}), \quad M_{A_H} = \frac{g'f}{\sqrt{5}}(1 - \frac{5v^2}{8f^2}), \quad (2)$$

with g and g' being the SM $SU(2)$ and $U(1)$ gauge couplings, respectively. The T-even W^\pm and Z bosons of the SM, whose masses at $\mathcal{O}(v^2/f^2)$ are given by

$$M_W = \frac{gv}{2}(1 - \frac{v^2}{12f^2}), \quad M_Z = \frac{gv}{2\cos\theta_W}(1 - \frac{v^2}{12f^2}), \quad M_A = 0. \quad (3)$$

Here, v represents the Higgs doublet VEV, which can be given by

$$v = \frac{f}{\sqrt{2}} \arccos \left(1 - \frac{v_{\text{SM}}^2}{f^2} \right) \simeq v_{\text{SM}} \left(1 + \frac{1}{12} \frac{v_{\text{SM}}^2}{f^2} \right), \quad (4)$$

where $v_{\text{SM}} = 246$ GeV is the SM Higgs VEV.

The implementation of T-parity in the fermion sector requires the introduction of mirror fermions. Then, the T-odd mirror partners for each SM fermions are added and one can write down a Yukawa-type interaction to give masses to the mirror fermions

$$\mathcal{L}_{\text{mirror}} = -\kappa_{ij} f (\bar{\Psi}_2^i \xi + \bar{\Psi}_1^i \Sigma_0 \Omega \xi^\dagger \Omega) \Psi_R^j + h.c. \quad (5)$$

where $i, j = 1, 2, 3$ are the generation indices. After EWSB, the mirror leptons acquire masses, given at $\mathcal{O}(v^2/f^2)$ by

$$m_{\ell_H^i} = \sqrt{2}\kappa_i f, \quad m_{\nu_H^i} = m_{\ell_H^i} (1 - \frac{v^2}{8f^2}), \quad (6)$$

where κ_i are the eigenvalues of the mass matrix κ .

As discussed in detail in Ref.[13], the existence of two Cabibbo-Kobayashi-Maskawa (CKM)-like unitary mixing matrices $V_{H\ell}$ and $V_{H\nu}$ is one of the important ingredients in the mirror lepton sector. Note that $V_{H\ell}$ and $V_{H\nu}$ are related through the Pontecorvo-Maki-Nakagata-Saki (PMNS) matrix:

$$V_{H\nu}^\dagger V_{H\ell} = V_{\text{PMNS}}^\dagger, \quad (7)$$

where in V_{PMNS} the Majorana phases are set to zero as no Majorana mass term has been introduced for right-handed neutrinos.

Follow Ref.[14], the matrix $V_{H\ell}$ can be parameterized with three mixing angles $\theta_{12}^\ell, \theta_{23}^\ell, \theta_{13}^\ell$ and three complex phases $\delta_{12}^\ell, \delta_{23}^\ell, \delta_{13}^\ell$

$$V_{H\ell} = \begin{pmatrix} c_{12}^\ell c_{13}^\ell & s_{12}^\ell c_{13}^\ell e^{-i\delta_{12}^\ell} & s_{13}^\ell e^{-i\delta_{13}^\ell} \\ -s_{12}^\ell c_{23}^\ell e^{i\delta_{12}^\ell} - c_{12}^\ell s_{23}^\ell s_{13}^\ell e^{i(\delta_{13}^\ell - \delta_{23}^\ell)} & c_{12}^\ell c_{23}^\ell - s_{12}^\ell s_{23}^\ell s_{13}^\ell e^{i(\delta_{13}^\ell - \delta_{12}^\ell - \delta_{23}^\ell)} & s_{23}^\ell c_{13}^\ell e^{-i\delta_{23}^\ell} \\ s_{12}^\ell s_{23}^\ell e^{i(\delta_{12}^\ell + \delta_{23}^\ell)} - c_{12}^\ell c_{23}^\ell s_{13}^\ell e^{i\delta_{13}^\ell} & -c_{12}^\ell s_{23}^\ell e^{i\delta_{23}^\ell} - s_{12}^\ell c_{23}^\ell s_{13}^\ell e^{i(\delta_{13}^\ell - \delta_{12}^\ell)} & c_{23}^\ell c_{13}^\ell \end{pmatrix} \quad (8)$$

For the Yukawa interactions of the down-type quarks and charged leptons, one of the possible effective Lagrangians [15] is given by

$$\mathcal{L}_{\text{down}} = \frac{i\lambda_d}{2\sqrt{2}} f \epsilon_{ij} \epsilon_{xyz} \left[(\bar{\Psi}'_2)_x \Sigma_{iy} \Sigma_{jz} X - (\bar{\Psi}'_1 \Sigma_0)_x \tilde{\Sigma}_{iy} \tilde{\Sigma}_{jz} \tilde{X} \right] d_R, \quad (9)$$

where $\Psi'_1 = (-\sigma_2 q_1, 0, 0_2)^T$, $\Psi'_2 = (0_2, 0, -\sigma_2 q_2)^T$, $i, j = 1, 2$ and $x, y, z = 3, 4, 5$. Here X transforms into \tilde{X} under T-parity, and it is a singlet under $SU(2)_i$ ($i = 1 - 2$) and its $U(1)_i$ ($i = 1 - 2$) charges are $(Y_1, Y_2) = (1/10, -1/10)$. Usually, there are two possible choices for X : $X = (\Sigma_{33})^{-1/4}$ (denoted as Case A) and $X = (\Sigma_{33}^\dagger)^{1/4}$ (denoted as Case B), where Σ_{33} is the $(3, 3)$ component of the non-linear sigma model field Σ . At order $\mathcal{O}(v_{SM}^4/f^4)$, the corresponding corrections to the Higgs couplings with respect to their SM values are given by ($d \equiv d, s, b, \ell_i^\pm$)

$$\begin{aligned} \frac{g_{h\bar{d}d}}{g_{h\bar{d}d}^{SM}} &= 1 - \frac{1}{4} \frac{v_{SM}^2}{f^2} + \frac{7}{32} \frac{v_{SM}^4}{f^4} & \text{Case A} \\ \frac{g_{h\bar{d}d}}{g_{h\bar{d}d}^{SM}} &= 1 - \frac{5}{4} \frac{v_{SM}^2}{f^2} - \frac{17}{32} \frac{v_{SM}^4}{f^4} & \text{Case B} \end{aligned} \quad (10)$$

III. BRANCHING RATIO FOR $h \rightarrow \mu\tau$ IN THE LHT MODEL

In the LHT model, the relevant Feynman diagrams of the decay $h \rightarrow \mu\tau$ at one-loop

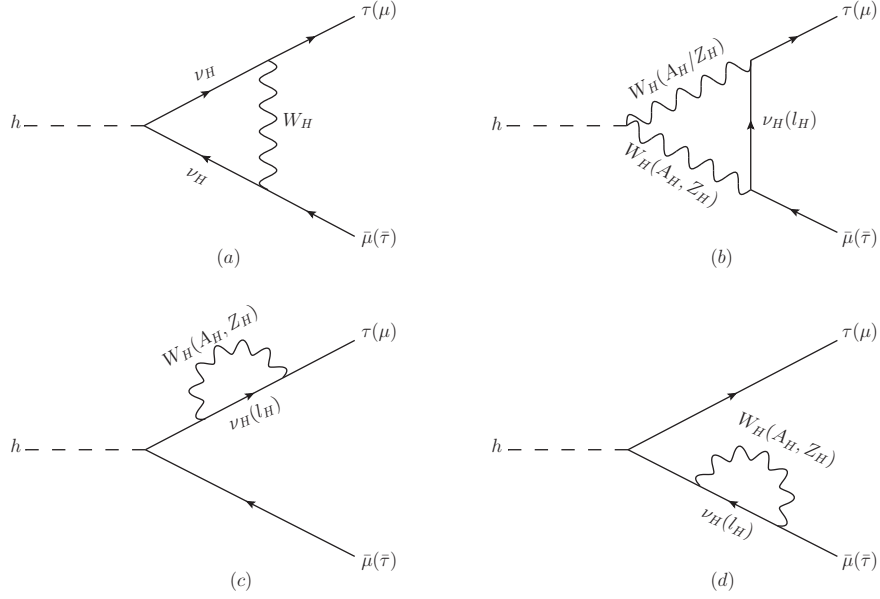


FIG. 1: Feynman diagrams of the decay $h \rightarrow \mu^\pm \tau^\mp$ at one-loop level in unitary gauge.

level in unitary gauge are shown in Fig.1, where the Goldstone bosons do not appear, Fig.1(a)(b) are vertex diagrams and Fig.1(c)(d) are self-energy diagrams. We can see that the flavor violating interactions between SM charged leptons and mirror leptons are mediated by the heavy gauge bosons A_H, Z_H, W_H^\pm . According to our calculation, we find that the contributions of the self-energy diagram and the contributions of the vertex diagram are at different order, i.e. $\Gamma_{\text{vertex}} \propto \mathcal{O}(v^2/f^2)\Gamma_{\text{self}}$. To be clear, we show the relevant Feynman rules and the explicit expressions of the $h \rightarrow \mu\bar{\tau}$ invariant amplitudes in Appendix A and Appendix B, respectively. This implies that the dominant contributions come from the self-energy diagrams, so we can calculate the invariant amplitude up to $\mathcal{O}(v/f)$ and ignore the contributions of the vertex diagram. We checked the divergence in the self-energy diagrams and found that the divergent terms have been canceled. Each loop diagram is composed of some scalar loop functions [16], which are calculated by using LoopTools[17].

In our numerical calculations, the SM parameters are taken as follows[18]

$$\begin{aligned} \sin^2 \theta_W &= 0.231, \quad \alpha_e = 1/128, \quad M_Z = 91.1876 \text{ GeV}, \\ m_\mu &= 105.66 \text{ MeV}, \quad m_\tau = 1776.82 \text{ MeV}, \quad m_h = 125 \text{ GeV}. \end{aligned} \quad (11)$$

The LHT parameters related to our calculations are the scale f , the Yukawa couplings

κ_i of the mirror neutrinos and the parameters in the matrices $V_{H\ell}, V_{H\nu}$. For the mirror neutrino masses, we assume

$$m_{\ell_H^1} = m_{\ell_H^2} = m_{\nu_H^1} = m_{\nu_H^2} = M_{12} = \sqrt{2}\kappa_{12}f, \quad m_{\ell_H^3} = m_{\nu_H^3} = M_3 = \sqrt{2}\kappa_3f. \quad (12)$$

For the Yukawa couplings, the search for the mono-jet events at the LHC Run-1[20] give the constraint $\kappa_i \geq 0.6$. Considering the constraints in Ref.[19], we scan over the free parameters f , κ_{12} and κ_3 within the following region

$$500\text{GeV} \leq f \leq 2000\text{GeV}, \quad 0.6 \leq \kappa_{12} \leq 3, \quad 0.6 \leq \kappa_3 \leq 3.$$

For the parameters in the matrices $V_{H\nu}, V_{H\ell}$, we follow Ref.[21] to consider the two scenarios as follows

- Scenario I: $V_{H\nu} = \mathbf{I}, V_{H\ell} = V_{\text{PMNS}}^\dagger$;
- Scenario II: $V_{H\ell} = V_{\text{CKM}}$.

where the PMNS matrix[22] and CKM matrix[18] are given by

$$V_{\text{PMNS}} = \begin{pmatrix} 0.822_{-0.011}^{+0.010} & 0.547_{-0.015}^{+0.016} & 0.155 \pm 0.008 \\ 0.451_{-0.014}^{+0.014} & 0.648_{-0.014}^{+0.012} & 0.614_{-0.017}^{+0.019} \\ 0.347_{-0.014}^{+0.016} & 0.529_{-0.014}^{+0.015} & 0.774_{-0.015}^{+0.013} \end{pmatrix}, \quad (13)$$

$$V_{\text{CKM}} = \begin{pmatrix} 0.97427 \pm 0.00014 & 0.22536 \pm 0.00061 & 0.00355 \pm 0.00015 \\ 0.22522 \pm 0.00061 & 0.97344 \pm 0.00015 & 0.0414 \pm 0.0012 \\ 0.00886_{-0.00032}^{+0.00033} & 0.0405_{-0.0012}^{+0.0011} & 0.99914 \pm 0.00005 \end{pmatrix}. \quad (14)$$

Furthermore, we will consider the constraint from the global fit of the current Higgs data and the electroweak precision observables (EWPOs) [23] as shown in Fig.2.

In Fig.3, we show the branching ratios of $h \rightarrow \mu\tau$ in the $\kappa_3 \sim f$ plane for two scenarios with excluded regions of Case A and Case B, where the $h \rightarrow \mu\bar{\tau}$ and $h \rightarrow \tau\bar{\mu}$ modes have been summed. From the left panel of Fig.4, we can see that the branching ratio of $h \rightarrow \mu\tau$ in scenario I can reach about 2×10^{-4} at 2σ level for Case A, which will become larger for Case B. From the right panel of Fig.3, we can see that the branching ratio of $h \rightarrow \mu\tau$ in scenario II can reach over 4×10^{-7} at 2σ level, which is three orders of magnitude smaller than the one in scenario I. We can see that the behaviors for two scenarios are

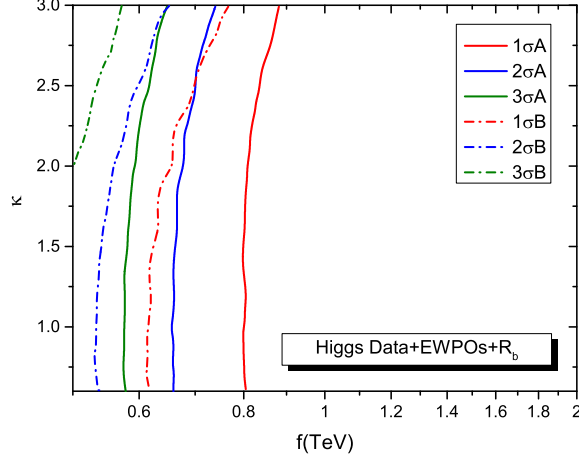


FIG. 2: Excluded regions (above each contour) in the $\kappa \sim f$ plane of the LHT model for Case A and Case B, where the parameter R is marginalized over. The solid (dash) lines from right to left respectively correspond to 1σ , 2σ and 3σ exclusion limits for Case A(Case B).

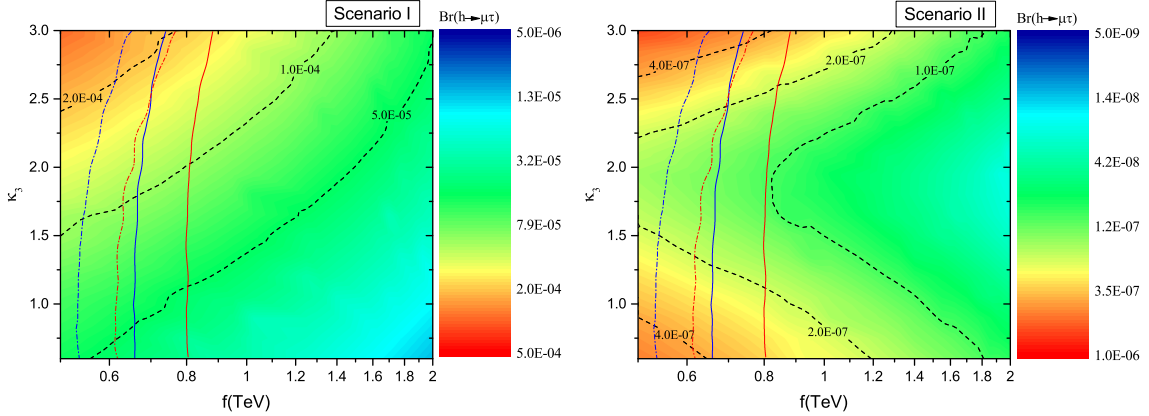


FIG. 3: Branching ratios of $h \rightarrow \mu\tau$ in the $\kappa_3 \sim f$ plane for two scenarios with excluded regions of Case A and Case B, respectively. The red lines and blue lines respectively correspond to 1σ and 2σ exclusion limits as shown in Fig.2.

very different due to the different selection of the matrix $V_{H\ell}$. From the two panels of Fig.3, we can see that the large branching ratios mainly lie in the upper-left corner for scenario I and upper-left or lower-left corners for scenario II, where the scale f is small and the Yukawa coupling κ_3 is either too large or too small.

In Fig.4, we show the branching ratios of $h \rightarrow \mu\tau$ in the $|M_3 - M_{12}| \sim f$ plane for two scenarios, respectively. We can see that the branching ratio of $h \rightarrow \mu\tau$ is insensitive to the mass splitting $|M_3 - M_{12}|$ values for scenario I. The largest branching ratios lie in

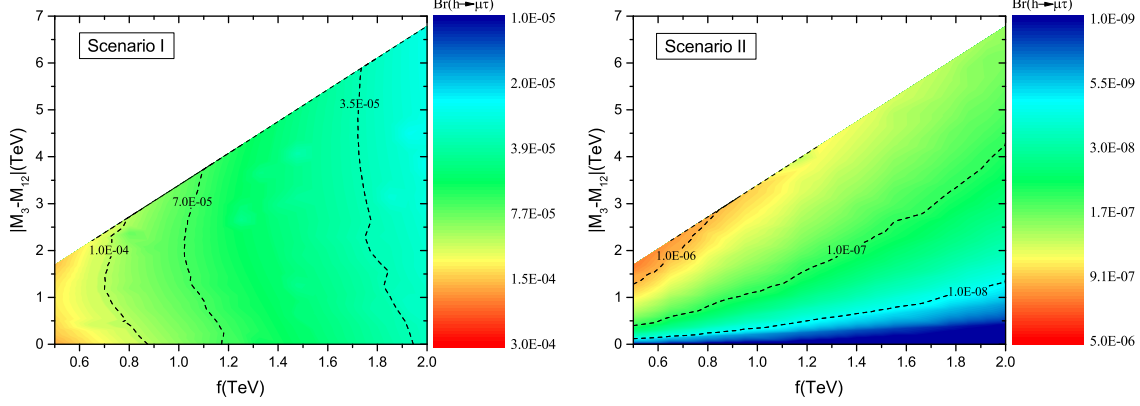


FIG. 4: Branching ratios of $h \rightarrow \mu\tau$ in the $|M_3 - M_{12}| \sim f$ plane for two scenarios.

the region of the contour figure with small f and $|M_3 - M_{12}|$ of $0 \sim 2$ TeV. For scenario II, we can see that the branching ratio of $h \rightarrow \mu\tau$ is enhanced by the increasing mass splitting $|M_3 - M_{12}|$. The largest branching ratios lie in the upper-left of the contour figure with small f and $|M_3 - M_{12}|$ of $1 \sim 2$ TeV.

IV. CORRELATION BETWEEN $h \rightarrow \mu\tau$, $\tau \rightarrow \mu\gamma$ AND $Z \rightarrow \mu\tau$

The upper limits on the LFV processes $\tau \rightarrow \mu\gamma$ and $Z \rightarrow \mu\tau$ are set: $\text{Br}(\tau \rightarrow \mu\gamma) < 4.4 \times 10^{-8}$ [24], $\text{Br}(Z \rightarrow \mu\tau) < 1.69 \times 10^{-5}$ [25], which may further strengthen the bounds on the branching ratios of $h \rightarrow \mu\tau$.

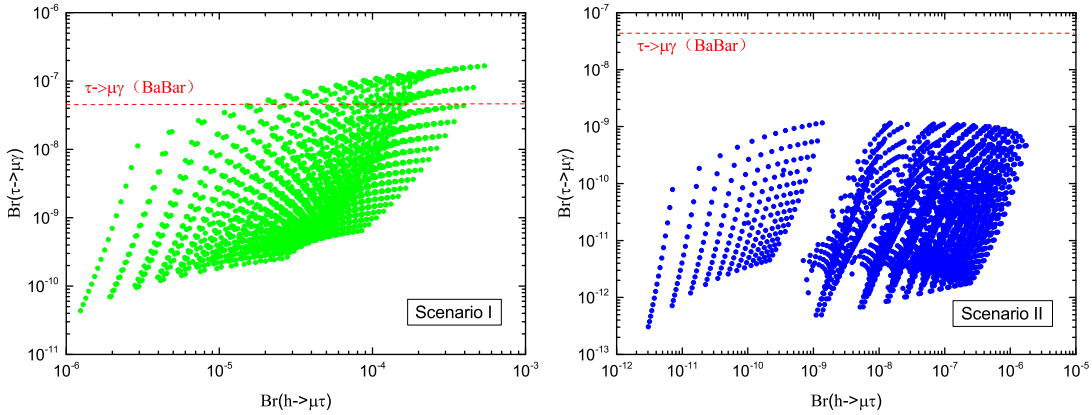


FIG. 5: Correlation between $\text{Br}(h \rightarrow \mu\tau)$ and $\text{Br}(\tau \rightarrow \mu\gamma)$ for two scenarios.

In Fig.5, we show the correlation between $\text{Br}(h \rightarrow \mu\tau)$ and $\text{Br}(\tau \rightarrow \mu\gamma)$ in two scenarios. The $\text{Br}(\tau \rightarrow \mu\gamma)$ can easily be obtained from Eq.(3.21) in Ref.[26], where we take

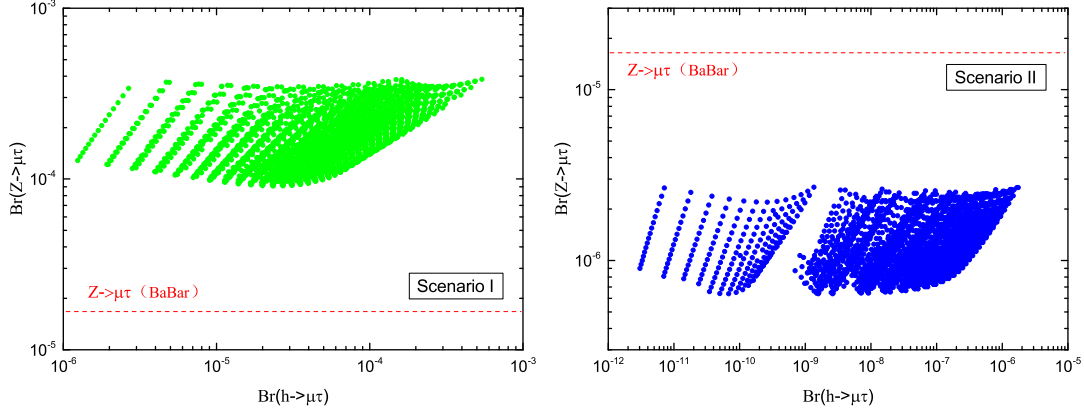


FIG. 6: Correlation between $\text{Br}(h \rightarrow \mu\tau)$ and $\text{Br}(Z \rightarrow \mu\tau)$ for two scenarios.

$\text{Br}(\tau^- \rightarrow \nu_\tau \mu^- \bar{\nu}_\mu) = (17.41 \pm 0.04)\%$, and few other studies on such processes can be found in Ref.[27]. In Scenario I, we can see that a minority of points is outside the allowed range, which implies that the $V_{H\ell}$ matrix must be more hierarchical than V_{PMNS} in order to satisfy the present upper bounds on $h \rightarrow \mu\tau$ and $\tau \rightarrow \mu\gamma$. In Scenario II, we can see that all the points are in allowed range, this is because V_{CKM} matrix is much more hierarchical than V_{PMNS} .

In Fig.6, we show the correlation between $\text{Br}(h \rightarrow \mu\tau)$ and $\text{Br}(Z \rightarrow \mu\tau)$ in two scenarios. The partial Z decay width $\Gamma(Z \rightarrow \mu\tau)$ can be calculated by using LoopTools, the relevant Feynman diagrams can be found in Refs.[28]. In Scenario I, we can see that all the points violate the current experimental bounds and the great majority of points exceed $\mathcal{O}(10^{-4})$. This will require that the $V_{H\ell}$ matrix must be more hierarchical than V_{PMNS} , unless the mirror lepton masses are quasi-degenerate. In Scenario II, we can see that all the points satisfy the current upper bounds due to the large hierarchy of the V_{CKM} matrix.

V. CONCLUSIONS

In this paper, we calculated LFV Higgs decay $h \rightarrow \mu\tau$ at one-loop level in the LHT model. According to the parameters in the mixing matrices, we considered two scenarios and found that the branching ratios for $h \rightarrow \mu\tau$ can respectively reach $\mathcal{O}(10^{-4})$ and $\mathcal{O}(10^{-7})$ under the current experimental constraints. We also investigated the correlation

between $h \rightarrow \mu\tau$, $\tau \rightarrow \mu\gamma$ and $Z \rightarrow \mu\tau$, and found that the $Z \rightarrow \mu\tau$ can give a substantial constraint on the $h \rightarrow \mu\tau$, which required that the $V_{H\ell}$ matrix must have a very different hierarchy from V_{PMNS} matrix.

Acknowledgement

We thank Lei Wu, Qinghong Cao and Junjie Cao for helpful suggestions and discussions. This work is supported by the National Natural Science Foundation of China (NNSFC) under grant Nos. 11405047, 11305049, by Specialized Research Fund for the Doctoral Program of Higher Education under Grant No. 20134104120002, by the Startup Foundation for Doctors of Henan Normal University under Grant Nos. 11112 and qd15207, and by the Education Department Foundation of Henan Province(14A140010).

Appendix A: Feynman rules

Interaction	Feynman rule	Interaction	Feynman rule
$H\bar{\nu}_H^j\nu_H^j$	$i\frac{m_{\nu_H^j}}{v}\frac{v^2}{4f^2}$	$HA_{H\alpha}A_{H\beta}$	$-\frac{i}{2}g'^2vg_{\alpha\beta}$
$\bar{\ell}_H^jA_{H\alpha}\ell^k$	$-\frac{ig'}{10}(V_{H\ell})_{jk}\gamma_\alpha P_L$	$HZ_{H\alpha}Z_{H\beta}$	$-\frac{i}{2}g^2vg_{\alpha\beta}$
$\bar{\ell}_H^jZ_{H\alpha}\ell^k$	$\frac{ig}{2}(V_{H\ell})_{jk}\gamma_\alpha P_L$	$HA_{H\alpha}Z_{H\beta}$	$-\frac{i}{2}g'gvg_{\alpha\beta}$
$\bar{\nu}_H^jW_{H\alpha}^+\ell^k$	$-\frac{ig}{\sqrt{2}}(V_{H\ell})_{jk}\gamma_\alpha P_L$	$HW_{H\alpha}^+W_{H\beta}^-$	$-\frac{i}{2}g^2vg_{\alpha\beta}$

Appendix B: The expression of the $h \rightarrow \mu\bar{\tau}$ invariant amplitudes

They can be represented in form of 1-point, 2-point and 3-point standard functions A, B_0, B_1, C_{ij} . Here the momenta p_μ, p_τ are assumed to be outgoing.

(1) The vertex diagram contribution:

$$\begin{aligned}
\Gamma_{(a)}^{W_H\nu_H} &= -\frac{g^2}{2}(V_{H\ell})_{j2}(V_{H\ell})_{j3}^*\frac{m_{\nu_H^j}^2}{4f^2}\frac{v}{16\pi^2}\frac{i}{16\pi^2} \\
&[4C_\beta\gamma^\beta + 2C_0(\not{p}_\mu - \not{p}_\tau) + \frac{2}{m_{W_H}^2}\tilde{C}_\beta\gamma^\beta + \frac{1}{m_{W_H}^2}C_{\beta\alpha}\gamma^\beta(\not{p}_\mu - \not{p}_\tau)\gamma^\alpha]P_L \\
C_\beta &= C_\beta(p_\mu, -p_h, m_{W_H}, m_{\nu_H^j}, m_{\nu_H^j}), \\
\tilde{C}_\beta &= p_{\mu\beta}[-B_0(-p_h, m_{\nu_H^j}, m_{\nu_H^j}) + m_{W_H}^2C_{11}] - p_{h\beta}[B_1(-p_h, m_{\nu_H^j}, m_{\nu_H^j}) + m_{W_H}^2C_{12}]
\end{aligned} \tag{15}$$

$$\begin{aligned}
\Gamma_{(b)}^{W_H W_H} &= \frac{g^2}{2} \frac{g^2 v}{2} (V_{H\ell})_{j2} (V_{H\ell})_{j3}^* \frac{i}{16\pi^2} \\
&[2C_\beta \gamma^\beta + \frac{2}{m_{W_H}^2} \tilde{C}_\beta \gamma^\beta - \frac{m_{\nu_H^j}^4}{m_{W_H}^4} C_\beta \gamma^\beta - \frac{1}{m_{W_H}^4} (\tilde{B}_\beta \gamma^\beta - \gamma^\beta \not{p}_\mu \gamma^\nu B_{\mu\nu} + m_{\nu_H^j}^2 B_\beta \gamma^\beta)] P_L \quad (16) \\
B_\beta &= B_\beta(-p_h, m_{W_H}, m_{W_H}), \tilde{B}_\beta = -p_{h\beta} [m_{W_H}^2 B_1 - A_0(m_{W_H})], \\
C_\beta &= C_\beta(p_\mu, -p_h, m_{\nu_H^j}, m_{W_H}, m_{W_H}), \\
\tilde{C}_\beta &= p_{\mu\beta} [-B_0(-p_h, m_{W_H}, m_{W_H}) + m_{\nu_H^j}^2 C_{11}] - p_{h\beta} [B_1(-p_h, m_{W_H}, m_{W_H}) + m_{\nu_H^j}^2 C_{12}]
\end{aligned}$$

$$\begin{aligned}
\Gamma_{(b)}^{A_H A_H} &= \frac{g'^2}{100} \frac{g'^2 v}{2} (V_{H\ell})_{j2} (V_{H\ell})_{j3}^* \frac{i}{16\pi^2} \\
&[2C_\beta \gamma^\beta + \frac{2}{m_{A_H}^2} \tilde{C}_\beta \gamma^\beta - \frac{m_{\ell_H^j}^4}{m_{A_H}^4} C_\beta \gamma^\beta - \frac{1}{m_{A_H}^4} (\tilde{B}_\beta \gamma^\beta - \gamma^\beta \not{p}_\mu \gamma^\nu B_{\mu\nu} + m_{\ell_H^j}^2 B_\beta \gamma^\beta)] P_L \quad (17) \\
B_\beta &= B_\beta(-p_h, m_{A_H}, m_{A_H}), \tilde{B}_\beta = -p_{h\beta} [m_{A_H}^2 B_1 - A_0(m_{A_H})], \\
C_\beta &= C_\beta(p_\mu, -p_h, m_{\ell_H^j}, m_{A_H}, m_{A_H}), \\
\tilde{C}_\beta &= p_{\mu\beta} [-B_0(-p_h, m_{A_H}, m_{A_H}) + m_{\ell_H^j}^2 C_{11}] - p_{h\beta} [B_1(-p_h, m_{A_H}, m_{A_H}) + m_{\ell_H^j}^2 C_{12}]
\end{aligned}$$

$$\begin{aligned}
\Gamma_{(b)}^{A_H Z_H} &= \frac{g'^2}{20} \frac{g^2 v}{2} (V_{H\ell})_{j2} (V_{H\ell})_{j3}^* \frac{i}{16\pi^2} \\
&[-2C_\beta \gamma^\beta - \frac{1}{m_{A_H}^2} \tilde{C}_\beta \gamma^\beta - \frac{1}{m_{Z_H}^2} \tilde{C}_\beta \gamma^\beta + \frac{m_{\ell_H^j}^4}{m_{A_H}^2 m_{Z_H}^2} C_\beta \gamma^\beta \\
&+ \frac{1}{m_{A_H}^2 m_{Z_H}^2} (\tilde{B}_\beta \gamma^\beta - \gamma^\beta \not{p}_\mu \gamma^\nu B_{\mu\nu} + m_{\ell_H^j}^2 B_\beta \gamma^\beta)] P_L \quad (18) \\
B_\beta &= B_\beta(-p_h, m_{A_H}, m_{Z_H}), \tilde{B}_\beta = -p_{h\beta} [m_{A_H}^2 B_1 - A_0(m_{Z_H})], \\
C_\beta &= C_\beta(p_\mu, -p_h, m_{\ell_H^j}, m_{A_H}, m_{Z_H}), \\
\tilde{C}_\beta &= p_{\mu\beta} [-B_0(-p_h, m_{A_H}, m_{Z_H}) + m_{\ell_H^j}^2 C_{11}] - p_{h\beta} [B_1(-p_h, m_{A_H}, m_{Z_H}) + m_{\ell_H^j}^2 C_{12}]
\end{aligned}$$

$$\begin{aligned}
\Gamma_{(b)}^{Z_H A_H} &= \frac{g'^2}{20} \frac{g^2 v}{2} (V_{H\ell})_{j2} (V_{H\ell})_{j3}^* \frac{i}{16\pi^2} \\
&[-2C_\beta \gamma^\beta - \frac{1}{m_{A_H}^2} \tilde{C}_\beta \gamma^\beta - \frac{1}{m_{Z_H}^2} \tilde{C}_\beta \gamma^\beta + \frac{m_{\ell_H^j}^4}{m_{A_H}^2 m_{Z_H}^2} C_\beta \gamma^\beta \\
&+ \frac{1}{m_{A_H}^2 m_{Z_H}^2} (\tilde{B}_\beta \gamma^\beta - \gamma^\beta \not{p}_\mu \gamma^\nu B_{\mu\nu} + m_{\ell_H^j}^2 B_\beta \gamma^\beta)] P_L \quad (19) \\
B_\beta &= B_\beta(-p_h, m_{Z_H}, m_{A_H}), \tilde{B}_\beta = -p_{h\beta} [m_{Z_H}^2 B_1 - A_0(m_{A_H})], \\
C_\beta &= C_\beta(p_\mu, -p_h, m_{\ell_H^j}, m_{Z_H}, m_{A_H}), \\
\tilde{C}_\beta &= p_{\mu\beta} [-B_0(-p_h, m_{Z_H}, m_{A_H}) + m_{\ell_H^j}^2 C_{11}] - p_{h\beta} [B_1(-p_h, m_{Z_H}, m_{A_H}) + m_{\ell_H^j}^2 C_{12}]
\end{aligned}$$

$$\begin{aligned}
\Gamma_{(b)}^{Z_H Z_H} &= \frac{g^2}{4} \frac{g^2 v}{2} (V_{H\ell})_{j2} (V_{H\ell})_{j3}^* \frac{i}{16\pi^2} \\
&[2C_\beta \gamma^\beta + \frac{2}{m_{Z_H}^2} \tilde{C}_\beta \gamma^\beta - \frac{m_{\ell_H^j}^4}{m_{Z_H}^4} C_\beta \gamma^\beta - \frac{1}{m_{Z_H}^4} (\tilde{B}_\beta \gamma^\beta - \gamma^\beta \not{p}_\mu \gamma^\nu B_{\mu\nu} + m_{\ell_H^j}^2 B_\beta \gamma^\beta)] P_L \quad (20) \\
B_\beta &= B_\beta(-p_h, m_{Z_H}, m_{Z_H}), \tilde{B}_\beta = -p_{h\beta} [m_{Z_H}^2 B_1 - A_0(m_{Z_H})], \\
C_\beta &= C_\beta(p_\mu, -p_h, m_{\ell_H^j}, m_{Z_H}, m_{Z_H}), \\
\tilde{C}_\beta &= p_{\mu\beta} [-B_0(-p_h, m_{Z_H}, m_{Z_H}) + m_{\ell_H^j}^2 C_{11}] - p_{h\beta} [B_1(-p_h, m_{Z_H}, m_{Z_H}) + m_{\ell_H^j}^2 C_{12}]
\end{aligned}$$

(2) **The self-energy diagram contribution:**

$$\begin{aligned}
\Gamma_{(c)}^{\mu A_H} &= \frac{g'^2}{100} \frac{m_\mu}{v} (V_{H\ell})_{j2} (V_{H\ell})_{j3}^* \frac{1}{p_\tau^2 - m_\mu^2} \frac{i}{16\pi^2} \\
&(2m_\mu B_\beta \gamma^\beta P_L + \frac{m_\mu}{m_{A_H}^2} \tilde{B}_\beta \gamma^\beta P_L - 2\not{p}_\tau B_\beta \gamma^\beta P_L - \frac{1}{m_{A_H}^2} \not{p}_\tau \tilde{B}_\beta \gamma^\beta P_L) \quad (21) \\
B_\beta &= B_\beta(p_\tau, m_{\ell_H^j}, m_{A_H}), \tilde{B}_\beta = p_{\tau\beta} [m_{\ell_H^j}^2 B_1 - A_0(m_{A_H})]
\end{aligned}$$

$$\begin{aligned}
\Gamma_{(c)}^{\mu Z_H} &= \frac{g^2}{4} \frac{m_\mu}{v} (V_{H\ell})_{j2} (V_{H\ell})_{j3}^* \frac{1}{p_\tau^2 - m_\mu^2} \frac{i}{16\pi^2} \\
&(2m_\mu B_\beta \gamma^\beta P_L + \frac{m_\mu}{m_{Z_H}^2} \tilde{B}_\beta \gamma^\beta P_L - 2\not{p}_\tau B_\beta \gamma^\beta P_L - \frac{1}{m_{Z_H}^2} \not{p}_\tau \tilde{B}_\beta \gamma^\beta P_L) \quad (22) \\
B_\beta &= B_\beta(p_\tau, m_{\ell_H^j}, m_{Z_H}), \tilde{B}_\beta = p_{\tau\beta} [m_{\ell_H^j}^2 B_1 - A_0(m_{Z_H})]
\end{aligned}$$

$$\begin{aligned}
\Gamma_{(c)}^{\mu W_H} &= \frac{g^2}{2} \frac{m_\mu}{v} (V_{H\ell})_{j2} (V_{H\ell})_{j3}^* \frac{1}{p_\tau^2 - m_\mu^2} \frac{i}{16\pi^2} \\
&(2m_\mu B_\beta \gamma^\beta P_L + \frac{m_\mu}{m_{W_H}^2} \tilde{B}_\beta \gamma^\beta P_L - 2\not{p}_\tau B_\beta \gamma^\beta P_L - \frac{1}{m_{W_H}^2} \not{p}_\tau \tilde{B}_\beta \gamma^\beta P_L) \quad (23) \\
B_\beta &= B_\beta(p_\tau, m_{\nu_H^j}, m_{W_H}), \tilde{B}_\beta = p_{\tau\beta} [m_{\nu_H^j}^2 B_1 - A_0(m_{W_H})]
\end{aligned}$$

$$\begin{aligned}
\Gamma_{(d)}^{\tau A_H} &= \frac{g'^2}{100} \frac{m_\tau}{v} (V_{H\ell})_{j2} (V_{H\ell})_{j3}^* \frac{1}{p_\mu^2 - m_\tau^2} \frac{i}{16\pi^2} \\
&(2m_\tau B_\beta \gamma^\beta P_L + \frac{m_\tau}{m_{A_H}^2} \tilde{B}_\beta \gamma^\beta P_L + 2B_\beta \gamma^\beta \not{p}_\mu P_R + \frac{1}{m_{A_H}^2} \tilde{B}_\beta \gamma^\beta \not{p}_\mu P_R) \quad (24) \\
B_\beta &= B_\beta(-p_\mu, m_{\ell_H^j}, m_{A_H}), \tilde{B}_\beta = -p_{\mu\beta} [m_{\ell_H^j}^2 B_1 - A_0(m_{A_H})]
\end{aligned}$$

$$\begin{aligned}
\Gamma_{(d)}^{\tau Z_H} &= \frac{g^2}{4} \frac{m_\tau}{v} (V_{H\ell})_{j2} (V_{H\ell})_{j3}^* \frac{1}{p_\mu^2 - m_\tau^2} \frac{i}{16\pi^2} \\
&(2m_\tau B_\beta \gamma^\beta P_L + \frac{m_\tau}{m_{Z_H}^2} \tilde{B}_\beta \gamma^\beta P_L + 2B_\beta \gamma^\beta \not{p}_\mu P_R + \frac{1}{m_{Z_H}^2} \tilde{B}_\beta \gamma^\beta \not{p}_\mu P_R) \quad (25) \\
B_\beta &= B_\beta(-p_\mu, m_{\ell_H^j}, m_{Z_H}), \tilde{B}_\beta = -p_{\mu\beta} [m_{\ell_H^j}^2 B_1 - A_0(m_{Z_H})]
\end{aligned}$$

$$\begin{aligned}
\Gamma_{(d)}^{\tau W_H} &= \frac{g^2 m_\tau}{2 v} (V_{H\ell})_{j2} (V_{H\ell})_{j3}^* \frac{1}{p_\mu^2 - m_\tau^2} \frac{i}{16\pi^2} \\
&\quad (2m_\tau B_\beta \gamma^\beta P_L + \frac{m_\tau}{m_{W_H}^2} \tilde{B}_\beta \gamma^\beta P_L + 2B_\beta \gamma^\beta \not{p}_\mu P_R + \frac{1}{m_{W_H}^2} \tilde{B}_\beta \gamma^\beta \not{p}_\mu P_R) \\
B_\beta &= B_\beta(-p_\mu, m_{\nu_H^j}, m_{W_H}), \tilde{B}_\beta = -p_{\mu\beta} [m_{\nu_H^j}^2 B_1 - A_0(m_{W_H})]
\end{aligned} \tag{26}$$

-
- [1] G. Aad et al.(ATLAS Collaboration), Phys. Lett. B 710, 49 (2012); S. Chatrchyan et al.(CMS Collaboration), Phys. Lett. B 710, 26 (2012).
- [2] see examples, A. Falkowski and R. Vega-Morales, JHEP 1412, 037 (2014), arXiv:1405.1095; D. Curtin *et al.*, Phys. Rev. D 90, no. 7, 075004 (2014), arXiv:1312.4992; C. Han, N. Liu, L. Wu, J. M. Yang and Y. Zhang, Eur. Phys. J. C 73, no. 12, 2664 (2013), arXiv:1212.6728; J. Cao, L. Wu, P. Wu and J. M. Yang, JHEP 1309, 043 (2013), arXiv:1301.4641; J. Huang, T. Liu, L. T. Wang and F. Yu, Phys. Rev. D 90, no. 11, 115006 (2014), arXiv:1407.0038; J. Cao, C. Han, L. Wu, J. M. Yang and M. Zhang, Eur. Phys. J. C 74, no. 9, 3058 (2014), arXiv:1404.1241; C. Han, X. Ji, L. Wu, P. Wu and J. M. Yang, JHEP 1404, 003 (2014), arXiv:1307.3790; S. L. Hu, N. Liu, J. Ren and L. Wu, J. Phys. G 41, no. 12, 125004 (2014), arXiv:1402.3050; L. Wu, JHEP 1502, 061 (2015), arXiv:1407.6113; D. Curtin and C. B. Verhaaren, JHEP 1512, 072 (2015), arXiv:1506.06141; L. Wu, J. M. Yang, C. P. Yuan and M. Zhang, Phys. Lett. B 747, 378 (2015) arXiv:1504.06932; A. Kobakhidze, L. Wu and J. Yue, JHEP 1410, 100 (2014), arXiv:1406.1961; JHEP 1604, 011 (2016), arXiv:1512.08922; H. Blusca-Maïto and A. Falkowski, arXiv:1602.02645.
- [3] V. Khachatryan et al. (CMS Collaboration), Phys. Lett. B 749, 337 (2015), arXiv:1502.07400.
- [4] G. Aad et al. (ATLAS Collaboration), JHEP 1511, 211 (2015), arXiv:1508.03372.
- [5] E. Arganda, M. J. Herrero, X. Marcano and C. Weiland, Phys. Rev. D 91, 015001 (2015); E. Arganda, A.M. Curiel, M.J. Herrero, D. Temes, Phys. Rev. D 71, 035011 (2005), hep-ph/0407302.
- [6] J. Cao, L. Wu and J. M. Yang, Nucl. Phys. B 829, 370 (2010); E. Arganda, M. J. Herrero, X. Marcano, C. Weiland, Phys. Rev. D 93, 055010 (2016), arXiv: 1508.04623; E. Arganda, M. J. Herrero, R. Morales and A. Szykman, JHEP 1603, 055 (2016), arXiv:1510.04685;

- A. Hammad, S. Khalil and C. Un, arXiv:1605.07567; M. Arana-Catania, E. Arganda, M.J. Herrero JHEP 1309, 160 (2013), arXiv:1304.3371.
- [7] A. Crivellin, G. D'Ambrosio, J. Heeck, Phys. Rev. Lett. 114, 151801 (2015); N. Bizot, S. Davidson, M. Frigerio, J. L. Kneur, JHEP 1603, 073 (2016); N. Bizot, S. Davidson, M. Frigerio, J. -L. Kneur, JHEP 1603, 073 (2016); F. J. Botella, G. C. Branco, M. Nebot, M. N. Rebelo, Eur. Phys. J. C 76, 161 (2016); D. Das and A. Kundu, Phys. Rev. D 92, 015009 (2015), arXiv:1504.01125; D. Aristizabal Sierra, A. Vicente, Phys. Rev. D 90, 115004 (2014), arXiv:1409.7690.
- [8] L. T. Hue, H. N. Long, T. T. Thuc and T. Phong Nguyen, Nucl. Phys. B 907, 37 (2016), arXiv:1512.03266.
- [9] S. Baek, Z.-F. Kang, JHEP 1603, 106 (2016); S. Baek, K. Nishiwaki, Phys. Rev. D 93, 015002 (2016); K. Cheung, W. Y. Keung, P. Y. Tseng, Phys. Rev. D 93, 015010 (2016); W. Altmannshofer, S. Gori, A. L. Kagan, L. Silvestrini, J. Zupan, Phys. Rev. D 93, 031301 (2016); X. G. He, J. Tandean, Y. J. Zheng, JHEP 1509, 093 (2015); I. Dorsner, S. Fajfer, A. Greljo, J. F. Kamenik, N. Kosnik, Ivan Nisandzic, JHEP 1506, 108 (2015); A. Crivellin, G. D'Ambrosio and J. Heeck, Phys. Rev. D 91, 075006 (2015); L. D. Lima, C. S. Machado, R. D. Matheus, L. A. F. D. Prado, JHEP 1511, 074 (2015); I. d. M. Varzielas, O. Fischer, V. Maurer, JHEP 1508, 080 (2015); C. F. Chang, C. H. V. Chang, C. S. Nugroho, T. C. Yuan, arXiv:1602.00680; C. H. Chen, T. Nomura, arXiv:1602.07519; K. Huitu, V. Keus, N. Koivunen, O. Lebedev, arXiv:1603.06614; M. Sher, K. Thrasher, Phys. Rev. D 93, 055021 (2016); A. Lami, P. Roig, Phys. Rev. D 94, 056001 (2016), arXiv:1603.09663; J. G. Koerner, A. Pilaftsis, K. Schilcher, Phys. Rev. D 47:1080-1086 (1993); A. Pilaftsis, Phys. Lett. B 285, 68-74(1992); J. Heeck, M. Holthausen, W. Rodejohann, Y. Shimizu, Nucl. Phys. B 896, 281-310(2015); J. Herrero-Garcia, N. Rius, A. Santamaria, JHEP 1611, 084(2016).
- [10] S. L. Glashow, J. Iliopoulos and L. Maiani, Phys. Rev. D 2, 1285 (1970).
- [11] A. Goyal, hep-ph/0609095; S.R. Choudhury, A.S. Cornell, A. Deandrea, N. Gaur and A. Goyal, Phys. Rev. D 75, 055011 (2007), hep-ph/0612327.
- [12] H. C. Cheng and I. Low, JHEP 0309, 051 (2003); JHEP 0408, 061 (2004); I. Low, JHEP 0410, 067 (2004); J. Hubisz and P. Meade, Phys. Rev. D 71, 035016 (2005).
- [13] J. Hubisz, S.J. Lee and G. Paz, JHEP 06, 041 (2006), hep-ph/0512169.

- [14] M. Blanke, et al., Phys. Lett. B 646, 253 (2007).
- [15] C. R. Chen, K. Tobe and C. P. Yuan, Phys. Lett. B 640, 263 (2006).
- [16] G. 't Hooft and M. J. G. Veltman, Nucl. Phys. B 153, 365 (1979).
- [17] T. Hahn and M. Perez-Victoria, Comput. Phys. Commun. 118, 153 (1999); T. Hahn, Nucl. Phys. Proc. Suppl. 135, 333 (2004).
- [18] K. A. Olive et al., (Particle Data Group), Chinese Physics C Vol. 38, No. 9 (2014) 090001.
- [19] B. F. Yang, X. L. Wang and J. Z. Han, Nucl. Phys. B 847, 1 (2011), arXiv:1103.2506; J. Hubisz, P. Meade, A. Noble and M. Perelstein, JHEP 0601, 135 (2006); A. Belyaev, C. R. Chen, K. Tobe and C. P. Yuan, Phys. Rev. D 74, 115020 (2006); Q. H. Cao and C. R. Chen, Phys. Rev. D 76, 075007 (2007); J. Reuter, M. Tonini, JHEP 0213,077 (2013); X. F. Han, L. Wang, J. M. Yang, J. Y. Zhu, Phys. Rev. D 87, 055004 (2013); J. Reuter, M. Tonini, M. de Vries, arXiv:1307.5010; C. C. Han, A. Kobakhidze, N. Liu, L. Wu and B. F. Yang, Nucl. Phys. B 890, 388 (2014), arXiv:1405.1498.
- [20] J. Hubisz, P. Meade, A. Noble and M. Perelstein, JHEP 01, 135 (2006); M. Perelstein, J. Shao, Phys. Lett. B 704, 510 (2011); G. Cacciapaglia, et al., Phys. Rev. D 87, 075006 (2013); J. Reuter, M. Tonini, M. de Vries, JHEP 1402, 053 (2014); J. Reuter, M. Tonini, JHEP 1302, 077 (2013).
- [21] H. S. Hou, Phys. Rev. D 75, 094010 (2007); J. Z. Han, B. Z. Li and X. L. Wang, Phys. Rev. D 83, 034032 (2011), arXiv:1102.4402.
- [22] Y. J. Zhang, X. Y. Zhang, B.-Q. Ma, Phys. Rev. D 86, 093019 (2012).
- [23] B. F. Yang, G. F. Mi, N. Liu, JHEP 1410, 47 (2014), arXiv:1407.6123; N. Liu, L. Wu, B. F. Yang and M.C. Zhang, Phys. Lett. B 753, 664 (2016), arXiv:1508.07116; B. F. Yang, Z. Y. Liu, N. Liu, arXiv:1603.04242.
- [24] K. Hayasaka et al. (Belle collaboration), Phys. Lett. B 666, 16-22 (2008); B. Aubert et al. (BABAR collaboration), Phys. Rev. Lett. 104, 021802 (2010).
- [25] ATLAS Collaboration, CERN-EP-2016-055, arXiv:1604.07730 [hep-ex].
- [26] M. Blanke, et al., JHEP 0705, 013 (2007).
- [27] T. Goto, Y. Okada, Y. Yamamoto, Phys. Rev. D 83, 053011 (2011).
- [28] J. Z. Han, X. L. Wang, B. F. Yang, Nucl. Phys. B 843, 383-395 (2011), arXiv:1101.3598; C.-X. Yue, J.-Y. Liu, and S.-H. Zhu, Phys. Rev. D 78, 095006 (2008).